The Astrophysical Journal Letters, 929:L16 (6pp), 2022 April 10 https://doi.org/10.3847/2041-8213/ac63a3
© 2022. The Author(s). Published by the American Astronomical Society.
OPEN ACCESS

New Constraint on Early Dark Energy from Planck and BOSS Data Using the Profile Likelihood

Laura Herold[1], Elisa G. M. Ferreira[1,2,3], and Eiichiro Komatsu[1,2]
[1] Max-Planck-Institut für Astrophysik, Karl-Schwarzschild-Str. 1, D-85748 Garching, Germany; lherold@mpa-garching.mpg.de, elisa.ferreira@ipmu.jp
[2] Kavli IPMU (WPI), UTIAS, The University of Tokyo, 5-1-5 Kashiwanoha, Kashiwa, Chiba 277-8583, Japan
[3] Instituto de Física, Universidade de São Paulo—C.P. 66318, CEP: 05315-970, São Paulo, Brazil
Received 2021 December 23; revised 2022 March 14; accepted 2022 April 4; published 2022 April 14

Abstract

A dark energy–like component in the early universe, known as early dark energy (EDE), is a proposed solution to the Hubble tension. Currently, there is no consensus in the literature as to whether EDE can simultaneously solve the Hubble tension and provide an adequate fit to the data from the cosmic microwave background (CMB) and large-scale structure of the universe. In this work, we deconstruct the current constraints from the Planck CMB and the full-shape clustering data of the Baryon Oscillation Spectroscopic Survey to understand the origin of different conclusions in the literature. We use two different analyses, a grid sampling and a profile likelihood, to investigate whether the current constraints suffer from volume effects upon marginalization and are biased toward some values of the EDE fraction, $f_{\rm EDE}$. We find that the $f_{\rm EDE}$ allowed by the data strongly depends on the particular choice of the other parameters of the model, and that several choices of these parameters prefer larger values of $f_{\rm EDE}$ than in the Markov Chain Monte Carlo analysis. This suggests that volume effects are the reason behind the disagreement in the literature. Motivated by this, we use a profile likelihood to analyze the EDE model and compute a confidence interval for $f_{\rm EDE}$, finding $f_{\rm EDE} = 0.072 \pm 0.036$ (68% C.L.). Our approach gives a confidence interval that is not subject to volume effects and provides a powerful tool to understand whether EDE is a possible solution to the Hubble tension.

Unified Astronomy Thesaurus concepts: Hubble constant (758); Cosmology (343); Cosmological parameters (339); Dark energy (351)

1. Introduction

Measurements of the Hubble constant, H_0, the present-day expansion rate of the universe, obtained with different techniques show a discrepancy known as the "Hubble tension" (Bernal et al. 2016). Indirect measurements, which depend on the assumption of a cosmological model, yield systematically lower values of H_0 than direct measurements, which do not or only weakly depend on the assumption of a cosmological model.

The most significant tension is seen between the (indirect) inference of H_0 from the cosmic microwave background (CMB) data of the Planck mission assuming a flat Λ cold dark matter (ΛCDM) cosmological model, $H_0 = 67.37 \pm 0.54$ km s^{-1} Mpc^{-1} (Planck Collaboration VI 2020), and the (direct) local inference from the Cepheid-calibrated Type Ia supernovae of the SH0ES project, $H_0 = 73.04 \pm 1.04$ km s^{-1} Mpc^{-1} (Riess et al. 2021). The statistical significance of the tension is 5σ. Throughout this paper, we quote uncertainties at the 68% confidence level (C.L.), unless noted otherwise.

This tension could hint at new physics beyond the flat ΛCDM model. One of the proposed models to alleviate the tension is early dark energy (EDE; Poulin et al. 2018, 2019; Smith et al. 2020). In this model, the ΛCDM cosmology is extended to include a dark energy–like component in the pre-recombination era, which reduces the size of the sound horizon and increases H_0 (Bernal et al. 2016). EDE is typically parameterized by three parameters: the initial value of the EDE field (θ_i), its maximum fractional energy density ($f_{\rm EDE}$), and the critical redshift (z_c) at which this maximum fraction is reached.

EDE was shown to reduce the tension between the values of H_0 (Poulin et al. 2018; Smith et al. 2020) inferred from the CMB data of Planck (Planck Collaboration XI 2016), the baryon acoustic oscillation (BAO) and redshift-space distortion data of the Baryon Oscillation Spectroscopic Survey (BOSS; Alam et al. 2017), the BAO measurements from the 6 Degree Field Galaxy Survey (Beutler et al. 2011) and Sloan Digital Sky Survey Main Galaxy Sample (Ross et al. 2015), the Pantheon supernova sample (Scolnic et al. 2018), and the direct measurement by the SH0ES collaboration (Riess et al. 2019). They find $f_{\rm EDE} = 0.107^{+0.035}_{-0.030}$, which gives $H_0 = 71.49 \pm 1.20$ km s^{-1} Mpc^{-1}.

However, it was pointed out in Hill et al. (2020) that introducing EDE leads to a higher amplitude of matter density fluctuations parameterized by Ω_m and σ_8, worsening the so-called σ_8 tension. They showed that including further large-scale structure (LSS) probes such as the Dark Energy Survey (Abbott et al. 2018), Kilo-Degree Survey (Hildebrandt et al. 2020), and Hyper Suprime-Cam (Hikage et al. 2019), which are particularly sensitive to Ω_m and σ_8, weakens the evidence for EDE. When including all probes but H_0 from SH0ES, their analysis yields an upper limit of $f_{\rm EDE} < 0.06$ at 95% C.L. A similar constraint of $f_{\rm EDE} < 0.072$ at 95% C.L. (with $f_{\rm EDE} = 0.025^{+0.006}_{-0.025}$) is obtained when employing the full shape of the galaxy power spectrum combined with the BAO data of BOSS Data Release 12 (DR12) galaxies along with the Planck data (Ivanov et al. 2020a). Concurrently, a similar analysis from D'Amico et al. (2021) found $f_{\rm EDE} < 0.08$ at 95% C.L. for the same data set and including the Pantheon supernova

Original content from this work may be used under the terms of the Creative Commons Attribution 4.0 licence. Any further distribution of this work must maintain attribution to the author(s) and the title of the work, journal citation and DOI.

sample. These three papers conclude that EDE does not solve the Hubble tension.

In the analyses of Hill et al. (2020), Ivanov et al. (2020a), and D'Amico et al. (2021), all three EDE parameters $\{f_{\rm EDE}, \theta_i, z_c\}$ are varied, which is referred to as the "three-parameter model." Smith et al. (2021) argued that the reason for the small preferred value of $f_{\rm EDE}$ found by them is due to volume effects upon marginalization and proposed alternative approaches.[4] In particular, they found $f_{\rm EDE} = 0.072 \pm 0.034$ for the same data set as in Ivanov et al. (2020a) when fixing two EDE parameters $\{\theta_i, z_c\}$, which is referred to as the "one-parameter model."Within the one-parameter model, they observe that including LSS data decreases the evidence for EDE similar to the three-parameter model; they relate this tighter constraint on EDE to the lower clustering amplitude preferred by LSS data compared to CMB data. The one-parameter model was already explored earlier in Niedermann & Sloth (2020) in the context of new EDE.

Currently, there is no agreement in the community as to whether EDE can simultaneously solve the Hubble tension and fit all available data sets. A new chapter in this discussion was presented recently. Two groups (Hill et al. 2021; Poulin et al. 2021) independently reported on a 2σ–3σ preference for EDE when analyzing the model using the CMB data of the Atacama Cosmology Telescope (ACT; Choi et al. 2020). South Pole Telescope data (Dutcher et al. 2021) are consistent with both ACT and Planck results (Posta et al. 2021).

One question that remains open is, what is the reason behind this disagreement? The root of this seems to lie in the Markov Chain Monte Carlo (MCMC) sampling of the three parameters of the EDE model. For $f_{\rm EDE} = 0$, the EDE model is degenerate with ΛCDM for any choice of θ_i and z_c. Therefore, the parameter volume for $f_{\rm EDE} = 0$ is larger than for every $f_{\rm EDE} > 0$. This can lead to a preference for $f_{\rm EDE} = 0$ in the marginalized posterior, affecting the inferred amount of EDE allowed by the data. On the other hand, fixing some parameters of the model, as for the one-parameter model, is an incomplete analysis, as stated in Smith et al. (2021); the results might depend on the particular choice of the parameters.

In this paper, we deconstruct the current constraints on the EDE model from the CMB and BOSS full-shape clustering data. Our goal is to understand where the disagreement in the literature comes from and check if volume effects are indeed present. In particular, we answer the following questions. Is the three-parameter model affected by the two unconstrained parameters θ_i and z_c or volume effects? Do the results of the one-parameter model depend on the particular choice of θ_i and z_c, and how well can the results be generalized to the full three-parameter model? How would the constraints on $f_{\rm EDE}$ change if those effects were eliminated?

To this end, we perform two analyses: a grid sampling and a profile likelihood. With the grid sampling, we explore the parameter space of $\{\theta_i, z_c\}$ by fixing them to a wide range of values and performing the one-parameter analysis. This analysis shows that higher values of $f_{\rm EDE}$ are consistent with the data, which suggests that the three-parameter MCMC analysis is affected by volume effects, and that there is a strong dependence of $f_{\rm EDE}$ on the particular choice of $\{\theta_i, z_c\}$. This makes it difficult to generalize the results of the one-parameter model. To confirm the presence of volume effects, we perform a frequentist-statistic analysis using a profile likelihood. We find that a considerably larger $f_{\rm EDE}$ is preferred by the data compared to the Bayesian MCMC analysis, confirming that volume effects affect the three-parameter analysis.

The rest of this paper is organized as follows. In Section 2, we describe the EDE model. In Section 3, we deconstruct the current constraints using the grid and the profile likelihood. In Section 4, we construct a new confidence interval using the profile likelihood. We discuss the results and conclude in Section 5.

2. EDE Model

The idea behind early-time solutions to the Hubble tension is to reduce the sound horizon and hence increase the inferred value of H_0 (Bernal et al. 2016). The sound horizon, $r_s = \int_{z_*}^{\infty} c_s(z)\, dz \Big/ H(z)$, where z_* is the redshift of the last scattering surface, $c_s(z)$ is the sound speed in the baryon-photon plasma, and $H(z)$ is the expansion rate of the universe, is dominated by contributions near the lower bound of the integral.

EDE (Kamionkowski et al. 2014; Karwal & Kamionkowski 2016; Caldwell & Devulder 2018) is an extra component added to the energy density budget near z_*, which increases $H(z)$ and lowers r_s. This can be achieved by a pseudoscalar field, ϕ, which obeys the following requirements: (i) it starts becoming relevant at matter–radiation equality, (ii) it behaves like dark energy at early times, and (iii) its energy density dilutes faster than the matter density after z_*. To model this behavior, the canonical EDE model is given by the potential (Poulin et al. 2019)

$$V(\phi) = V_0[1 - \cos(\phi/f)]^n\,, \tag{1}$$

where $V_0 = m^2 f^2$, m is the mass of ϕ, and f is the spontaneous symmetry breaking scale.

The parameters of the model can be rewritten in terms of the phenomenological parameters $\{f_{\rm EDE}, \theta_i, z_c, n\}$, where $f_{\rm EDE}$ is the maximum fraction of EDE at the critical redshift z_c, and θ_i is the initial value of the dimensionless field, $\theta \equiv \phi/f$. A larger value of $f_{\rm EDE}$ leads to a higher H_0. To solve the Hubble tension, it was predicted that $f_{\rm EDE} \simeq 0.1$ would be necessary (Knox & Millea 2020).

The EDE field ϕ in a cosmological background with the potential given in Equation (1) behaves like dark energy initially, with the field essentially frozen. Once $H(z)$ becomes smaller than the effective mass $m_{\rm eff} = d^2V(\phi)/d\phi^2$, ϕ starts decaying and oscillating at the bottom of the potential with an effective, time-averaged equation-of-state parameter of $\langle w \rangle = (n-1)/(n+1)$. Here we choose $n = 3$ as in the previous analyses, which was shown to dilute sufficiently fast to satisfy the third requirement (Poulin et al. 2019; Smith et al. 2020).

3. Deconstructing the Current Constraints on the EDE Model

3.1. Data and Methodology

For our analysis, we use a similar setup as in Ivanov et al. (2020a). We combine the following publicly available extensions of the Einstein–Boltzmann solver `CLASS` (Blas et al. 2011; Lesgourgues 2011):[5] `CLASS_EDE` (Hill et al. 2020),

[4] An exploration of volume effects with an averaging method can be found in the Appendix of Ivanov et al. (2020a).

[5] The code used for this analysis is publicly available at https://github.com/LauraHerold/CLASS-PT_EDE.

which evolves the EDE field as a pseudoscalar field up to linear order in perturbations, and `CLASS-PT` (Chudaykin et al. 2020), which is based on the effective field theory (EFT) of LSS (Baumann et al. 2012; Carrasco et al. 2012) and allows one to model the galaxy power spectrum up to mildly nonlinear scales. We perform an MCMC inference with `MontePython` (Brinckmann & Lesgourgues 2018) using the Metropolis–Hastings algorithm (Metropolis et al. 1953; Hastings 1970).

Our data set consists of the Planck 2018 TT+TE+EE +lowℓ+lensing likelihoods (Planck Collaboration VI 2020) along with the BOSS DR12 full-shape likelihood based on the EFT of LSS presented in D'Amico et al. (2020) and Ivanov et al. (2020b). Note that this is a slightly different data set than in Ivanov et al. (2020a) and Smith et al. (2021), who also included the BOSS (reconstructed) BAO likelihood. We have checked that including the reconstructed BAO data in addition does not lead to a large change of our conclusions. Recently, there has been an update on the BOSS window function from Beutler & McDonald (2021) that might impact the conclusions in the previous analysis cited here. To compare with the published constraints, we do not use the new window functions.

We sample the ΛCDM parameters ω_b, $\omega_{\rm CDM}$, θ_s, A_s, n_s, and $\tau_{\rm reio}$ assuming flat priors, along with the Planck and EFT nuisance parameters. In Section 3.2, we assume $f_{\rm EDE} \in [0.001, 0.5]$, and in Sections 3.3 and 4, we assume $\theta_i \in [0.1, 3.1]$ and $\log(z_c) \in [3, 4.3]$. Following the convention of the Planck collaboration (Planck Collaboration VI 2020), we model the neutrino sector by two massless and one massive neutrino species with $m_\nu = 0.06$ eV.

3.2. Grid Sampling

In this section, we perform our first analysis to study how much the conclusions of Smith et al. (2021) drawn from the one-parameter model depend on the particular choice of $\theta_i = 2.775$ and $\log(z_c) = 3.569$. An exploration of the effect of θ_i, z_c on cosmological observables can be found in Smith et al. (2020), Poulin et al. (2019), and Lin et al. (2019).

The potential problem encountered in the MCMC exploration of the three-parameter model is a preference for small $f_{\rm EDE}$ due to volume effects upon marginalization over θ_i and z_c. We investigate this problem as follows. To explore the dependence of the $f_{\rm EDE}$ constraints on θ_i and z_c, we run several MCMC inferences, where we keep θ_i and z_c fixed to different values and vary only $f_{\rm EDE}$. We choose six values in the typical prior range of $\theta_i \in [0.1, 3.1]$ and seven values in the typical prior range of $\log(z_c) \in [3, 4.3]$:

$$\theta_i = \{0.3, 0.8, 1.3, 1.8, 2.3, 2.8\},$$
$$\log(z_c) = \{3.1, 3.3, 3.5, 3.7, 3.9, 4.1, 4.3\}.$$

Throughout this paper, log denotes the logarithm with base 10. This gives a 6×7 grid of MCMC analyses. For each MCMC, we infer the mean fraction of EDE, $\bar{f}_{\rm EDE}$, depending on the choice of θ_i and z_c. We run every MCMC until the Gelman–Rubin convergence criterion $R - 1 < 0.1$ is reached. Our results are summarized in Figure 1.

We find that $\bar{f}_{\rm EDE}$ strongly depends on the particular choice of θ_i and $\log(z_c)$. There are choices of θ_i and $\log(z_c)$ that allow for higher $f_{\rm EDE}$. For example, $\theta_i = 2.8$ and $\log(z_c) = 3.5$ (which are close to the values chosen by Smith et al. 2021, $\theta_i = 2.775$ and $\log(z_c) = 3.569$) allow for particularly high $f_{\rm EDE} = 0.057^{+0.027}_{-0.034}$, the highest found in the grid. The authors pointed out that this choice of $\{\theta_i, z_c\}$ is reasonable, since it is obtained from the best-fit cosmology to Planck data. However, for $\theta_i = 1.8$ and $\log(z_c) = 3.7$ (which are similar to the mean values found in Ivanov et al. 2020a, $\theta_i = 2.023$ and $\log(z_c) = 3.71$), we find $f_{\rm EDE} = 0.017^{+0.004}_{-0.016}$. This shows that the particular choice of θ_i and $\log(z_c)$ made in Smith et al. (2021) is the reason for a higher $f_{\rm EDE}$ than found in Ivanov et al. (2020a). We point out that the best-fit and mean values quoted in Ivanov et al. (2020a; best-fit values $\theta_i = 2.734$ and $\log(z_c) = 3.52$) correspond to choices of θ_i and $\log(z_c)$ that allow for high and low values of $f_{\rm EDE}$, respectively.

We also explore the dependence of the best-fit $f_{\rm EDE}$ and the $\Delta\chi^2$ as a function of θ_i and z_c in Appendix A, finding a similar pattern as in Figure 1. We show that the choice of $\theta_i = 2.8$ and $\log(z_c) = 3.5$, which gives the highest mean and best fit of $f_{\rm EDE}$, has the smallest χ^2.

As the constraint on $f_{\rm EDE}$ depends strongly on the particular choice of $\{\theta_i, z_c\}$, the analysis of the one-parameter model presented in Smith et al. (2021) might have been biased. Our result also shows that, if $\{\theta_i, z_c\}$ cannot be constrained, as in the MCMC analysis of the three-parameter model (Ivanov et al. 2020a), it might lead to misleading constraints on $f_{\rm EDE}$.

Our grid method is not plagued by volume effects, since there is no larger prior volume at $f_{\rm EDE} = 0$ compared to $f_{\rm EDE} > 0$ when θ_i and $\log(z_c)$ are fixed. This coarse-grained exploration of the $\{\theta_i, z_c\}$ parameter space made with the grid shows that higher values of $f_{\rm EDE}$ are allowed for a considerable part of the parameter space and present a good fit to the data. This indicates that volume effects might be present in the three-parameter MCMC analysis and that, when this effect is eliminated, the preference for a smaller $f_{\rm EDE}$ in the posterior is weakened.

Motivated by this, in the next section, we perform a frequentist analysis using profile likelihoods, which does not suffer from volume effects.

3.3. Profile Likelihood

Comparison of the results obtained from Bayesian and frequentist analyses is useful for checking if priors or marginalization affect the results (Cousins 1995). A profile likelihood is a standard tool in frequentists' statistics. To construct a profile likelihood, one fixes the parameter of interest, i.e., in our case, $f_{\rm EDE}$, to different values and maximizes the likelihood $\mathcal{L}$ (or minimizes $\chi^2 = -2\ln\mathcal{L}$) with respect to all of the other parameters of the model, i.e., all ΛCDM parameters, θ_i and z_c, as well as all nuisance parameters, for every choice of the parameter of interest ($f_{\rm EDE}$). The $\Delta\chi^2$ as a function of the parameter of interest is the profile likelihood (see, e.g., Planck Collaboration Int. XVI 2014, for an application to the Planck data).

For the minimization, we adopt the method used in Schöneberg et al. (2021). For every fixed value of $f_{\rm EDE}$, we first run a long MCMC (with at least 10^4 accepted steps) until the Gelman–Rubin criterion $R - 1 < 0.25$ is reached. This yields a reasonable estimate for the best-fit values and covariance of all other parameters. Second, we run three small chains with successively decreasing step size (decreasing temperature) and enhanced sensitivity to the likelihood difference. This is done with a slightly modified Metropolis–Hastings algorithm as described in Schöneberg et al. (2021). Since they found that in the context of EDE and other solutions

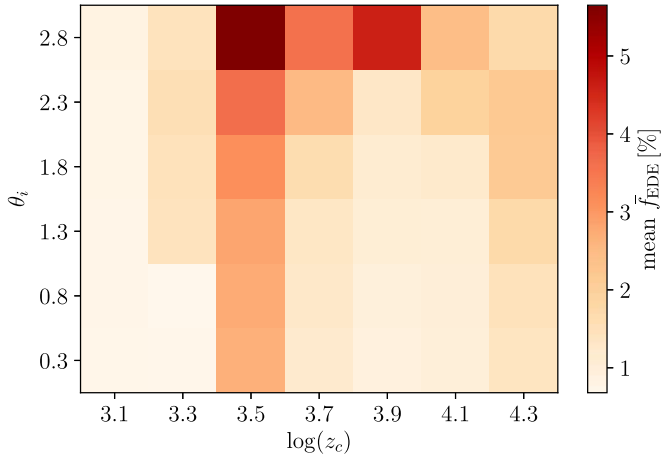

Figure 1. Mean values of $f_{\rm EDE}$ for different fixed values of θ_i and $\log(z_c)$. Every value in this 6×7 grid is determined by a full MCMC analysis.

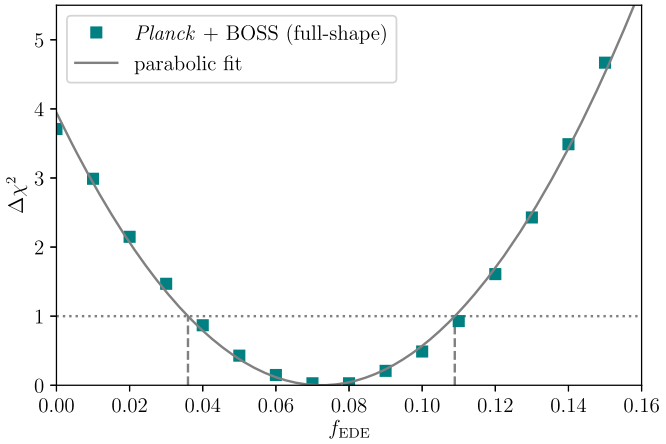

Figure 2. Profile likelihood of the fraction of EDE, $f_{\rm EDE}$, from the Planck CMB and the BOSS full-shape galaxy clustering data. We show $\Delta\chi^2 = -2\ln(\mathcal{L}/\mathcal{L}_{\rm max})$, where $\mathcal{L}_{\rm max}$ is the maximum likelihood (green markers) and a parabola fit (gray line). The confidence interval is constructed using the Feldman–Cousins prescription (Feldman & Cousins 1998; vertical dashed lines). It is indistinguishable from the interval constructed from the intersection of the parabola with $\Delta\chi^2 = 1$ (horizontal dotted line).

to the Hubble tension, this method was less likely to get stuck in local minima than algorithms based on gradient descent, such as MIGRAD (James & Roos 1975), we adopted the same approach.

The results of the minimization are shown as the markers in Figure 2. For a parameter following a Gaussian distribution, one would expect a parabola, which is a good fit for $f_{\rm EDE} < 0.15$ (gray line). The minimum of the curve is the minimum $\chi^2(f_{\rm EDE})$ and shows the best-fit value for $f_{\rm EDE}$. From the profile likelihood, one can already see that our best-fit value lies near the upper bound, $f_{\rm EDE} < 0.072$ (95% C.L.), of Ivanov et al. (2020a). This is a strong indication that the MCMC analysis of the three-parameter model is plagued by volume effects. The profile likelihood does not suffer from volume effects, since the minimum $\chi^2(f_{\rm EDE})$ is the same as the maximum-likelihood estimate.

We report the best-fit values of all parameters for $f_{\rm EDE} = 0$, 0.07, and 0.11 in Appendix B. We found that the best-fit values of $\{\theta_i, z_c\}$ are approximately constant for all fixed values of $f_{\rm EDE}$ and fluctuate within a few percent around $\log(z_c) = 3.56$ and $\theta_i = 2.75$. Note that these values are very close to the ones adopted in the one-parameter model in Smith et al. (2021).

4. Constructing Confidence Intervals: Profile Likelihood

To construct confidence intervals from the profile likelihood shown in Figure 2, we use the prescription introduced by Feldman & Cousins (1998), which is suitable for a parameter with a physical boundary like $f_{\rm EDE}$, which has to lie between zero and 1. The Feldman–Cousins prescription is based on the likelihood ratio

$$R(x) = \frac{\mathcal{L}(x|\mu)}{\mathcal{L}(x|\mu_{\rm best})}, \tag{2}$$

where x is the observable or measured value (it can take on all possible values for $f_{\rm EDE}$), μ is the true value of $f_{\rm EDE}$ (which will be read off at the minimum of the parabola), and $\mu_{\rm best}$ is the physically allowed value μ for which, for a given x, the likelihood $\mathcal{L}(x|\mu)$ is maximized; since $\mu_{\rm best} > 0$, it is $\mu_{\rm best} = x$ for $x \geqslant 0$ and $\mu_{\rm best} = 0$ for $x < 0$. The confidence interval $[x_1, x_2]$ is chosen such that $R(x_1) = R(x_2)$ and

$$\int_{x_1}^{x_2} \mathcal{L}(x|\mu)\,{\rm d}x = \alpha, \tag{3}$$

where α is the C.L., e.g., $\alpha = 0.6827$ for a 68.27% C.L. To shorten the notation, we denote 68.27% C.L. as 68% C.L. in the remainder of the paper. For a given μ, the integral is solved numerically and tabulated by Feldman & Cousins (1998). The Feldman–Cousins prescription unambiguously determines whether one parameter should be quoted as an upper/lower limit or a central confidence interval. Here we find a central confidence interval at the 68% C.L. By reading off μ at the minimum of the parabola shown in Figure 2, we find $f_{\rm EDE} = 0.072 \pm 0.036$ ($f_{\rm EDE} = 0.072^{+0.071}_{-0.060}$ at 95% C.L.).

The upper and lower bounds of the 68% confidence interval are shown in Figure 2 as the vertical dashed lines. They coincide with the confidence intervals constructed by the Neyman prescription (Neyman 1937; interval between parabola points that intersect with $\Delta\chi^2 = 1$), which is only valid far away from a physical boundary.

5. Discussion and Conclusion

In this paper, we used the grid sampling and profile-likelihood methods to understand the difference in the constraints on the EDE model reported in the literature (Ivanov et al. 2020a; D'Amico et al. 2021; Smith et al. 2021) using the Planck CMB and the BOSS full-shape galaxy clustering data. With the grid sampling, we showed that the inferred mean and best-fit values of $f_{\rm EDE}$ depend strongly on the values of $\{\theta_i, z_c\}$. This finding is relevant, since the posterior distributions in the full three-parameter model shown in Ivanov et al. (2020a, their Figure 5) indicate that θ_i and particularly z_c are poorly constrained by the Planck and BOSS data. Also, depending on the particular choice of $\{\theta_i, z_c\}$ made in the one-parameter model, one could draw different conclusions about the amount of EDE allowed by the data. The choice made in Smith et al. (2021) is an example of a choice that allows for a high value of $f_{\rm EDE}$ and therefore a larger effect on H_0. However, even for the choice $\theta_i = 2.8$ and $\log(z_c) = 3.5$, which gives the highest

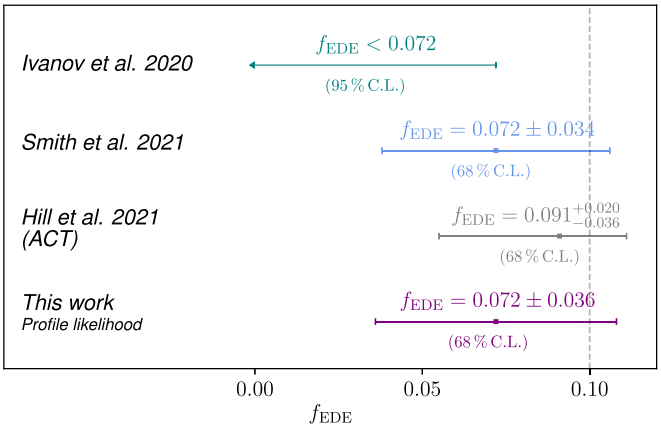

Figure 3. Summary of the current constraints on $f_{\rm EDE}$ from the Planck CMB and the BOSS full-shape galaxy clustering data by different methods: Ivanov et al. (2020a) with an MCMC inference of the three-parameter model in green (95% C.L.), Smith et al. (2021) with an MCMC inference within the one-parameter model in blue (68% C.L.), and our results obtained with the Feldman–Cousins prescription based on the profile likelihood in purple (68% C.L.). For comparison, we show the recent ACT results in gray (Hill et al. 2021; 68% C.L.). The vertical gray dashed line marks $f_{\rm EDE} = 0.1$.

value of $f_{\rm EDE}$ in our grid method, we find $H_0 = 69.52^{+0.95}_{-1.21}$ km s^{-1} Mpc^{-1}, which only partially alleviates the Hubble tension.

Based on the hints of the grid analysis, we constructed the profile likelihood for $f_{\rm EDE}$, which is not subject to volume effects upon marginalization in the MCMC chain. Using the Feldman–Cousins prescription, we constructed the confidence interval, finding $f_{\rm EDE} = 0.072 \pm 0.036$, providing a new and robust constraint on the EDE model.

In Figure 3, we compare the confidence interval from this work based on the profile likelihood to previous work. For reference, we mark $f_{\rm EDE} = 0.1$. Our best-fit value, $f_{\rm EDE} = 0.072$, is at the 95% confidence upper limit found in Ivanov et al. (2020a), which is $f_{\rm EDE} < 0.072$. This shows that there is an effect in the MCMC analysis that drives the constraint on $f_{\rm EDE}$ closer to zero. The most plausible explanation is volume effects upon marginalization due to the large prior volume in θ_i and z_c when $f_{\rm EDE} \to 0$. On the other hand, our best-fit value and the 68% C.L. are similar to those found in Smith et al. (2021), with the same central value and an only slightly larger confidence interval. Nevertheless, their result was obtained within the one-parameter model, which has a strong dependence on the particular choice of θ_i and z_c, as shown in Section 3.2, and cannot be used to draw conclusions about the full three-parameter model.

We suggest that the profile likelihood is a more suitable method to analyze the EDE model and determine $f_{\rm EDE}$. The confidence intervals obtained through this method do not suffer from volume effects or a reduced parameter space.

We did not construct confidence intervals for H_0 in this paper. This study is currently in progress, together with the analysis of the EDE model with different data sets.

We thank Paolo Campeti, Elisabeth Krause, Evan McDonough, Marta Monelli, Oliver Philcox, Fabian Schmidt, Sherry Suyu, and Sam Witte for useful discussions and suggestions. We also thank the organizers and participants of the Munich Institute for Astro- and Particle Physics (MIAPP) workshop "Accelerating Universe 2.0" for useful discussions about this project during the workshop. This work was supported in part by JSPS KAKENHI grant Nos. JP20H05850 and JP20H05859 and the Deutsche Forschungsgemeinschaft (DFG, German Research Foundation) under Germany's Excellence Strategy—EXC-2094-390783311. The Kavli IPMU is supported by the World Premier International Research Center Initiative (WPI), MEXT, Japan.

Appendix A
Best Fit and $\Delta\chi^2$ of Grid Analysis

The results of the grid analysis, showing the dependence of the best-fit $f_{\rm EDE}$ and $\Delta\chi^2$ as a function of θ_i and z_c, can be seen in Figure 4.

Appendix B
Best-fit Values of the Parameters for Different Cosmologies

In Table 1, we show the best-fit parameters obtained with the minimization described in Section 3.3 for the ΛCDM cosmology and EDE cosmologies with fixed $f_{\rm EDE}$. The first eight parameters in the table are varied in the MCMC, and the last six parameters are derived parameters. At the bottom, we quote the minimum χ^2. The cosmology with fixed $f_{\rm EDE} = 0.07$ is close to the best fit computed from the minimum of the parabola fit, and $f_{\rm EDE} = 0.11$ is at the higher end of the 68% confidence interval.

ORCID iDs

Laura Herold https://orcid.org/0000-0001-9054-1414
Elisa G. M. Ferreira https://orcid.org/0000-0002-5032-8368
Eiichiro Komatsu https://orcid.org/0000-0002-0136-2404

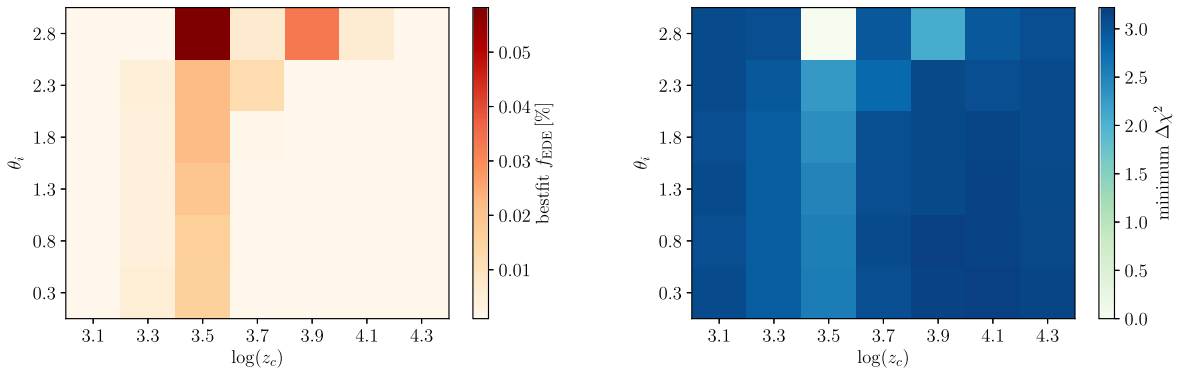

Figure 4. Best-fit values of $f_{\rm EDE}$ (left) and $\Delta\chi^2$ (right) for different fixed values of θ_i and $\log(z_c)$. Every value in this 6×7 grid is obtained with the minimization procedure described in Section 3.3.

Table 1
Best-fit Parameters for Different Cosmologies

Parameter	Best-fit ΛCDM	Best-fit $f_{\rm EDE} = 0.07$	Best-fit $f_{\rm EDE} = 0.11$
$100\,\omega_b$	2.245	2.259	2.270
$\omega_{\rm cdm}$	0.1191	0.1260	0.1304
$100 * \theta_s$	1.042	1.042	1.041
$\ln(10^{10}A_s)$	3.044	3.056	3.064
n_s	0.9681	0.9794	0.9872
$\tau_{\rm reio}$	0.0548	0.0549	0.0553
$\log(z_c)$	⋯	3.55	3.56
θ_i	⋯	2.76	2.77
$z_{\rm reio}$	7.701	7.827	7.924
$\Omega_{\rm m}$	0.3093	0.3046	0.3012
$Y_{\rm He}$	0.2454	0.2479	0.2480
H_0 [km s^{-1} Mpc^{-1}]	67.80	70.00	71.45
$10^{+9}A_s$	2.099	2.125	2.141
σ_8	0.808	0.825	0.836
Min. χ^2	3237.4	3233.7	3234.6

References

Abbott, T., Abdalla, F., Alarcon, A., et al. 2018, PhRvD, 98, 043526
Alam, S., Ata, M., Bailey, S., et al. 2017, MNRAS, 470, 2617
Baumann, D., Nicolis, A., Senatore, L., & Zaldarriaga, M. 2012, JCAP, 2012, 051
Bernal, J. L., Verde, L., & Riess, A. G. 2016, JCAP, 10, 019
Beutler, F., & McDonald, P. 2021, JCAP, 11, 031
Beutler, F., Blake, C., Colless, M., et al. 2011, MNRAS, 416, 3017
Blas, D., Lesgourgues, J., & Tram, T. 2011, JCAP, 2011, 034
Brinckmann, T., & Lesgourgues, J. 2018, PDU, 24, 100260
Caldwell, R. R., & Devulder, C. 2018, PhRvD, 97, 023532
Carrasco, J. J. M., Hertzberg, M. P., & Senatore, L. 2012, JHEP, 2012, 82
Choi, S. K., Hasselfield, M., Ho, S.-P. P., et al. 2020, JCAP, 2020, 045
Chudaykin, A., Ivanov, M. M., Philcox, O. H., & Simonović, M. 2020, PhRvD, 102, 063533
Cousins, R. D. 1995, AmJPh, 63, 398
Dutcher, D., Balkenhol, L., Ade, P., et al. 2021, PhRvD, 104, 022003
D'Amico, G., Gleyzes, J., Kokron, N., et al. 2020, JCAP, 2020, 005
D'Amico, G., Senatore, L., Zhang, P., & Zheng, H. 2021, JCAP, 2021, 072
Feldman, G. J., & Cousins, R. D. 1998, PhRvD, 57, 3873
Hastings, W. K. 1970, Biometrika, 57, 97
Hikage, C., Oguri, M., Hamana, T., et al. 2019, PASJ, 71, 43
Hildebrandt, H., Köhlinger, F., van den Busch, J. L., et al. 2020, A&A, 633, A69
Hill, J. C., McDonough, E., Toomey, M. W., & Alexander, S. 2020, PhRvD, 102, 043507
Hill, J. C., Calabrese, E., Aiola, S., et al. 2021, arXiv: 2109.04451
Ivanov, M. M., McDonough, E., Hill, J. C., et al. 2020a, PhRvD, 102, 103502
Ivanov, M. M., Simonović, M., & Zaldarriaga, M. 2020b, JCAP, 2020, 042
James, F., & Roos, M. 1975, CoPhC, 10, 343
Kamionkowski, M., Pradler, J., & Walker, D. G. E. 2014, PhRvL, 113, 251302
Karwal, T., & Kamionkowski, M. 2016, PhRvD, 94, 103523
Knox, L., & Millea, M. 2020, PhRvD, 101, 043533
Lesgourgues, J. 2011, arXiv: 1104.2932
Lin, M.-X., Benevento, G., Hu, W., & Raveri, M. 2019, PhRvD, 100, 063542
Metropolis, N., Rosenbluth, A. W., Rosenbluth, M. N., Teller, A. H., & Teller, E. 1953, JChPh, 21, 1087
Neyman, J. 1937, RSPTA, 236, 333
Niedermann, F., & Sloth, M. S. 2020, PhRvD, 102, 063527
Planck Collaboration Int. XVI 2014, A&A, 566, A54
Planck Collaboration VI 2020, A&A, 641, A6
Planck Collaboration XI 2016, A&A, 594, A11
Posta, A. L., Louis, T., Garrido, X., & Hill, J. C. 2021, arXiv: 2112.10754
Poulin, V., Smith, T. L., & Bartlett, A. 2021, PhRvD, 104, 123550
Poulin, V., Smith, T. L., Grin, D., Karwal, T., & Kamionkowski, M. 2018, PhRvD, 98, 083525
Poulin, V., Smith, T. L., Karwal, T., & Kamionkowski, M. 2019, PhRvL, 122, 221301
Riess, A. G., Casertano, S., Yuan, W., Macri, L. M., & Scolnic, D. 2019, ApJ, 876, 85
Riess, A. G., Yuan, W., Macri, L. M., et al. 2021, arXiv: 2112.04510
Ross, A. J., Samushia, L., Howlett, C., et al. 2015, MNRAS, 449, 835
Schöneberg, N., Abellán, G. F., Sánchez, A. P., et al. 2021, arXiv: 2107.10291
Scolnic, D. M., Jones, D. O., Rest, A., et al. 2018, ApJ, 859, 101
Smith, T. L., Poulin, V., & Amin, M. A. 2020, PhRvD, 101, 063523
Smith, T. L., Poulin, V., Bernal, J. L., et al. 2021, PhRvD, 103, 123542